Microstructural Characterization of Doped Gadolinia under Heavy-Ion Irradiation by Combined XRD and Raman Approaches

Hakjun Lee¹, Hyeongjin Kim¹, Ho Jin Ryu^{1*}, Seunghyeon Lee²
1 Department of Nuclear and Quantum Engineering, KAIST, Daehak-ro 291, Yuseong-gu, Daejeon, 34141, Korea 2 Heavy Ion Irradiation Facility, KAERI, 111 Daedeokdae-ro 989gil, Daejeon, 34057, Korea *Corresponding author: hojinryu@kaist.ac.kr

*Keywords: Burnable Absorber, Accident-tolerant fuel (ATF), Irradiation Behavior

1. Introduction

For advanced nuclear reactors such as SMRs, MSRs, and high-temperature gas-cooled reactors (HTGRs), design strategies are increasingly moving toward reducing or eliminating soluble boron for reactivity control. This shift addresses issues related to the positive Moderator Temperature Coefficient (MTC) and delayed reactivity feedback inherent to boric acid usage. One promising alternative is the incorporation of solid burnable absorbers directly into the fuel, as proposed in the Centered Self-Shielded Burnable Absorber (CSBA) concept. Within this approach, gadolinia (Gd $_2$ O $_3$) has emerged as a strong candidate due to its high neutronabsorption cross section and compatibility with ceramic fuel matrices.

Building upon our earlier investigation of undoped and doped gadolinia compositions under argon heavyion irradiation, this study expands the scope by introducing quantitative X-ray Diffraction (XRD) analysis and Raman spectroscopy to evaluate irradiationinduced structural changes in greater detail. Doped gadolinia samples were selected to address the inherent solubility challenges of pure gadolinia, microstructural responses were systematically characterized as a function of the displacement-per-atom (dpa) dose.

The XRD results, combined with Reference Intensity Ratio (RIR) analysis, enabled quantitative estimation of phase fractions in doped gadolinia compositions containing two or more distinct phases. This approach allowed a clearer comparison of how irradiation influenced the relative stability of each phase across different doping strategies. In parallel, Raman spectroscopy provided depth-resolved profiles that revealed variations in the microstructural state, as reflected in shifts and changes in specific vibrational frequency ranges. Together, these results offered direct insight into both the quantitative and spatial aspects of irradiation-induced changes in doped gadolinia ceramics.

2. Methods and Experimental Setups

In this section, experimental techniques and procedures that can assure precise reproduction are described.

2.1 Sample Preparation & Irradiation Experiment

Ceramic samples were prepared by powder mixing and sintering to achieve a a theoretical density of roughly 95%. Consequently, small coin-shaped gadolinia pellets (sample 1) with diameters of 3-4mm and thicknesses within 1mm were fabricated, with one side finely polished to facilitate the investigation.

The argon ion irradiation experiment was conducted at the KAERI-affiliated KAHIF (KAERI Heavy Ion Irradiation Facility). an Ar9+ ion beam with an energy of 6.8MeV was irradiated at an elevated temperature of 400 °C.

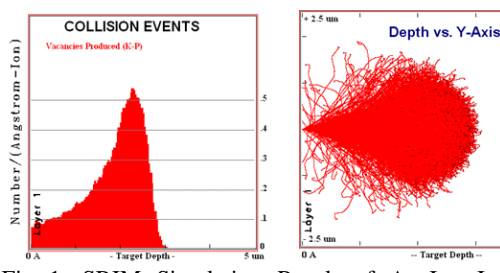


Fig 1. SRIM Simulation Result of Ar Ion Irradiated in Gadolinia. (a) Calculated depth-dpa profiles which can be seen on (b) the visualized trajectory of each simulated Ar ion

As a pre-assessment for actual ion irradiation, assessment of the depth-damage profile from the irradiation is simulated by SRIM 2008. From the figure above, the range corresponding to the maximum displacement damage (dpa) can be identified. According to the SRIM calculation results for gadolinia-based specimens, this range was approximately 2.3μm, and beyond a depth of about 3μm, radiation effects were predicted to be negligible. Finally, in the actual beam irradiation experiment, bundles of specimens with different gadolinia-based component compositions, were irradiated by Ar⁹⁺ ions of 3.7cm² beam area and an average current of 15μA for durations of 30, 100, and 300 minutes, respectively.

2.2 X-Ray Diffraction Specifications

The microstructures of irradiated specimens were examined using advanced characterization techniques available at the KAIST Analysis Center for Research Advancement (KARA). X-ray diffraction measurements

were carried out in both θ – 2θ and grazing-incidence configurations with a SmartLabTM High Resolution Thin-Film Diffractometer (RIGAKU) equipped with a Cu-K α radiation source. Scans were performed over a 10– 80° 2θ range at a speed of 4° /min. Grazing-incidence geometry, in particular, was employed to evaluate the surface-phase evolution in the irradiated ceramic samples, providing enhanced sensitivity to shallow irradiation-induced modifications.

2.3 Raman Spectroscopy

Raman spectroscopy was performed using a MarqMetrix All-in-One Raman analyzer (Thermo Fisher Scientific) to evaluate irradiation-induced changes in local bonding level. Measurements were carried out with a penetration depth of up to approximately 6 μm , using a step size of 0.4 μm to provide depth-resolved information on the irradiated layer. This configuration enabled not only the identification of characteristic peaks but also mapping of spectral variations across different depths. In particular, peaks around 266, 386, and 420 cm $^{-1}$ were closely examined, and their shifts and intensity changes were used to visualize microstructural modifications in doped gadolinia specimens.

3. Results and Discussions

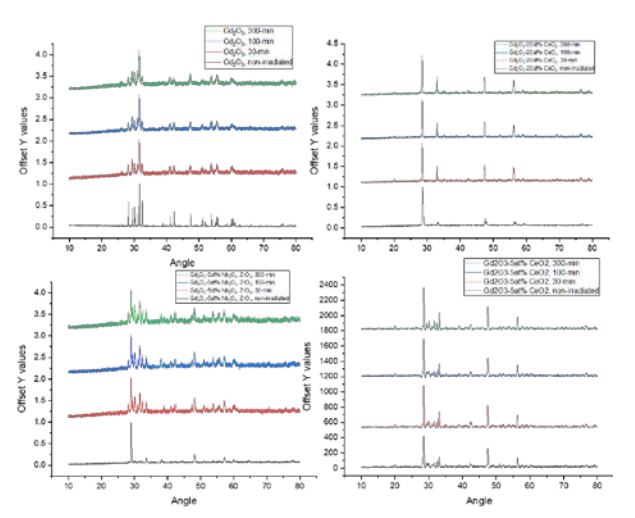


Fig 2. XRD peak patterns of four irradiated samples (a) pure gadolinia, (b) Gd_2O_3-20 at% CeO_2 , (c) Gd_2O_3-5 at% $Nb_2O_5ZrO_2$ and (d) Gd_2O_3-5 at% CeO_2 .

As shown on Fig 2(a), the XRD patterns of a pure gadolinia specimen sintered at about 1600 °C and the same specimen after a certain irradiation time. Considering the theoretical background that the monoclinic phase is more stable above 1200 °C, the pristine gadolinia (black line) shows peak patterns almost perfectly matching those of PDF card No. 00-042-1465 (Quality: S). After irradiation, slight peak broadening and an elevation in the low-angle region can be observed.

In contrast, when 20 at% CeO₂ was added to gadolinia, as seen in (b), the specimen exhibited only the four major peaks characteristic of cubic gadolinia even before irradiation, and it retained its cubic-phase tendency after irradiation. However, in some component samples, both monoclinic and cubic phases appeared simultaneously, and after ion irradiation, a rapid increase in the intensity of monoclinic peaks was observed.

Fig 2(c) shows the peaks of Gd_2O_3 –5 at% Nb_2O_5 and ZrO_2 , where distinct monoclinic peaks characteristic of the $28-33^{\circ}$ and $40-60^{\circ}$ ranges were clearly observed after irradiation compared to before, indicating that a phase transformation had occurred within the specimen.

Fig 2 (d), unlike (b), corresponds to a specimen with only 5% CeO₂ added to gadolinia. Here, the features of both cubic and monoclinic peaks are simultaneously present, and the peak intensities remain stable before and after irradiation without significant differences. For specimens containing both phases, multi-peak RIR analysis will be employed to investigate whether phase-fraction changes occur as a function of irradiation dose.

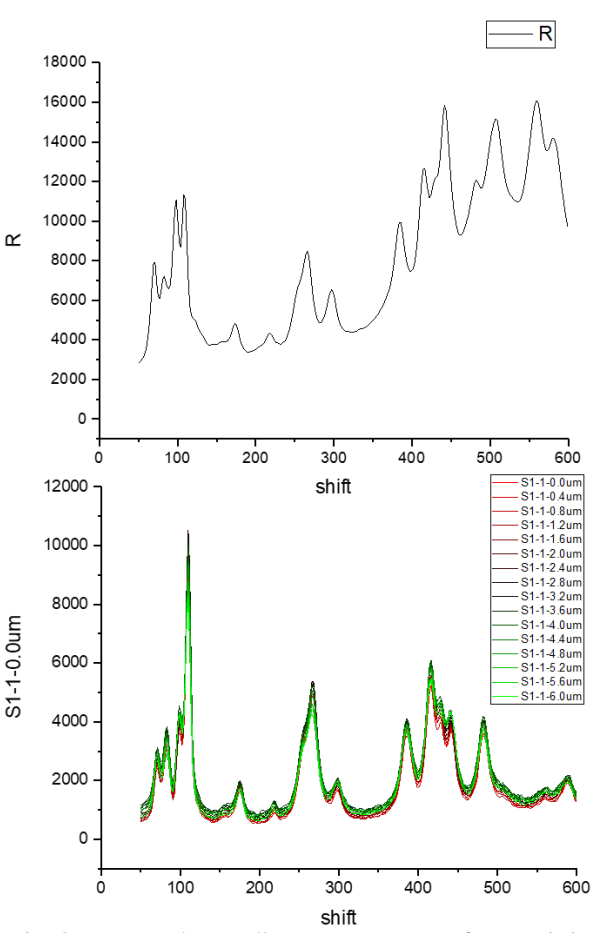


Fig 3. Measured overall Raman spectra of (a) pristine monoclinic (b) 30-min irradiated Gadolinia

Figure 3 (a) shows the Raman spectra of monoclinic gadolinia before and after irradiation. To visualize depth-dependent variations, 16 spectra were recorded from the surface down to a depth of $6.0\mu m$ in $0.4\mu m$ increments, with the line color gradually varied from bright red

(surface) to black and then light green (6.0 μ m depth). Considering the theoretically calculated radiation damage region shown in Fig. 1, the spectra between 1.5 and 2.5 μ m depth, represented by the dark red curves, correspond to the region most strongly affected by the primary collision cascades induced by irradiation.

According to SRIM theoretical calculations, Ar-ion collisions occur within a maximum depth of about $2.6~\mu m$. However, in Fig. 3 (b), the spectra corresponding to deeper regions (dark green to light green) still deviate significantly from the pristine specimen. This suggests that, even in the absence of direct collisions by Ar ions, secondary collision cascades generated deeper defects than SRIM predictions, or alternatively, point defects generated near the surface progressively diffused into the lattice, leading to accumulated distortion beyond $3~\mu m$.

The peaks showing notable changes before and after irradiation include those near 110, 266, 414, 428, and in the 550–600 cm⁻¹ range. Among these, the most striking feature is the sharp decrease in intensity around 550–600 cm⁻¹. This spectral region is associated with increased sublattice disorder and amorphization [3], which also corresponds well with the low-angle hump observed in the irradiated gadolinia XRD patterns in Fig. 2 (a). Furthermore, with increasing irradiation dose, the full width at half maximum (FWHM) of the 266 cm⁻¹ peak increases, indicating a rise in the non-uniformity of strain distribution within the lattice.[4]

A more detailed and quantitative analysis of each peak, along with additional studies of doped gadolinia specimens, will be performed in future work. In particular, unlike pure gadolinia with a monoclinic phase, doped gadolinia exhibiting cubic or mixed monoclinic—cubic phases will be analyzed further to discuss their irradiation-induced microstructural responses during the presentation.

4. Conclusions

In this study, we investigated the irradiation-induced microstructural evolution of undoped and doped gadolinia specimens using complementary XRD and Raman spectroscopy. The combination of RIR-based XRD analysis and depth-resolved Raman measurements enabled a quantitative evaluation of phase fractions and the visualization of defect-related vibrational changes. Undoped gadolinia showed strong agreement with the monoclinic reference phase, with irradiation leading to peak broadening and low-angle elevation. In contrast, doped compositions exhibited varying stability: Cedoped gadolinia maintained cubic characteristics, while Nb- and Zr-doped samples revealed clear monoclinic transformations. Raman spectra further confirmed sublattice disorder and strain accumulation, particularly in the 266 and 550-600 cm⁻¹ regions. Together, these results highlight the critical influence of doping on irradiation tolerance and phase stability, and provide a foundation for evaluating gadolinia-based absorbers in next-generation reactor applications.

REFERENCES

- [1] Nguyen, Xuan Ha, ChiHyung Kim, and Yonghee Kim. "An advanced core design for a soluble-boron-free small modular reactor ATOM with centrally-shielded burnable absorber." Nuclear Engineering and Technology 51.2 (2019): 369-376.
- [2] Oliver Werzer et al. "X-ray diffraction under grazing incidence conditions" nature reviews methods primers (2024) 4:15
- [3] Mishra, Maneesha; Kuppusami, P.; Ramya, S.; Ganesan, V.; Singh, Akash; Thirumurugesan, R.; Mohandas, E. "Microstructure and optical properties of Gd₂O₃ thin films prepared by pulsed laser deposition." Surface and Coatings Technology 262 (2015): 56–63.
- [4] Paul, N.; Devi, M.; Mohanta, D. "Synthesis, characterization and effect of low energy Ar ion irradiation on gadolinium oxide nanoparticles." Materials Research Bulletin 46.8 (2011): 1296–1300.